Princeton Plasma Physics Laboratory

PPPL- 4586

PPPL- 4586

Equilibrium and Stability of Partial Toroidal Plasma Discharges

E. Oz, C. E. Myers, M. Yamada, H. Ji, R. Kulsrud, and J. Xie

January, 2011

PPPL
PRINCETON PLASMA
PHYSICS LABORATORY

Prepared for the U.S. Department of Energy under Contract DE-AC02-09CH11466.

Princeton Plasma Physics Laboratory
Report Disclaimers

Full Legal Disclaimer

Trademark Disclaimer

PPPL Report Availability

Princeton Plasma Physics Laboratory:

http://www.pppl.gov/techreports.cfm

Office of Scientific and Technical Information (OSTI):

http://www.osti.gov/bridge

Related Links:

U.S. Department of Energy

Office of Scientific and Technical Information

Fusion Links

Equilibrium and Stability of Partial Toroidal Plasma Discharges

E. Oz,* C. E. Myers, M. Yamada,† H. Ji, R. Kulsrud, and J. Xie‡
Princeton Plasma Physics Laboratory, Princeton, NJ 08543, USA
(Dated: December 7, 2010)

The equilibrium and stability of partial toroidal flux ropes are studied in detail in the laboratory, motivated by ubiquitous loop structures on the solar surface. The flux ropes studied here are magnetized arc discharges formed in the Magnetic Reconnection Experiment (MRX). It is found that these loops robustly maintain their equilibrium on time scales much longer than the Alfvén time over a wide range of plasma current, guide field strength, and angle between electrodes, even in the absence of a strapping field. Additionally, the external kink stability of these flux ropes is found to be governed by the Kruskal-Shafranov limit for a flux rope with line-tied boundary conditions at both ends ($q > 1$).

Current loops or magnetic flux ropes are ubiquitous structures on the solar surface. Energetic activity such as Coronal Mass Ejections (CME) [e.g. 2] are often regarded as a consequence of instability and/or loss of equilibrium of such current loops. Theoretically, various models have been proposed to illustrate the dynamics of these current loops under specific geometries and boundary conditions where the field lines are considered anchored or "line-tied" to the photosphere [3–7]. However, despite rapid progress in observational capabilities of solar magnetic activity, none of these models have been tested conclusively due to lack of detailed magnetic measurements in crucial areas of the solar corona.

In contrast to remote-sensing observations, laboratory experiments offer *in situ* measurements that can be quantitatively compared to theoretical predictions. For periodic boundary conditions, the external kink stability of a current-carrying cylinder is governed by the Kruskal-Shafranov (KS) limit [8, 9] which is often expressed in terms of the so-called "safety factor,"

$$q = \frac{(2\pi a)^2 B_T}{\mu_0 I_p L_p} > 1, \tag{1}$$

where a is the radius of the cylinder, B_T is the guide (toroidal) magnetic field, I_p is the plasma current along the cylinder and L_p is the length. The KS theory has been quite successful in explaining stability of toroidal laboratory plasmas, such as tokamaks [10], which are appropriate for periodic boundary conditions.

It is not obvious, however, if the KS theory is directly applicable to solar current loops, which do not have periodic boundary conditions. Extensions of the KS theory have been made to take into account different boundary conditions [11–13]. The stability condition remains the same ($q > 1$) if both ends of the flux rope are line-tied (where displacements vanish), but the stability condition changes to $q > 2$ if one end is line-tied and the other end is free (where stresses vanish). Quantitative experimental tests of these predictions are available only recently using discharges between two electrically conducting electrodes in linear geometries, but with contradicting results. On one hand, clear stability conditions consistent with line-tied boundary conditions were observed as a part of spheromak formation [14] or in screw pinch discharges [15]. On the other hand, stability conditions consistent with one end line-tied and the other end free or partially free were also reported from another linear screw pinch experiment [16, 17]. In order to apply these results to astrophysical plasmas such as coronal flux loops, however, we must establish the conditions under which line-tied stability can be studied in the laboratory. The partial toroidal flux ropes studied here are found to consistently obey the line-tied $q > 1$ Kruskal-Shafranov limit over a wide range of plasma current, guide field stength, and angle between the electrodes.

The equilibrium of line-tied partial-toroidal flux ropes is also of great interest. Previous experiments have been conducted with flux rope discharges over a planar surface in the presence of a variable strapping field [18]. Based on images from a fast camera, it was found that a minimum strapping field is required to maintain the equilibrium. More recently, in a different set of experiments, it was found that when such equilibria are driven to erupt, they are always blown away, though in this case the loss of equilibrium is not current driven [19]. Thus, the crucial qualitative and quantitative questions regarding the equilibrium of current loops remain unanswered. With the flux ropes studied here, we find that the loop is able to robustly maintain its equilibiruim on time scales much longer than the Alfvén time, and that the loop is never blown away, regardless of the strapping field strength.

The new experiments reported here have been conducted in the Magnetic Reconnection Experiment (MRX) facility [1]. In order to form the partial toroidal flux rope, an arc discharge is created between two circular electrodes of equal size that are separated by a variable toroidal angle (see Fig. 1). The electrodes are copper disks of minor radius $a = 7.3$ cm. Their major radius R can be varied from 20 to 30 cm, and the angle between them Θ can be varied from 90° to 270° (Fig. 1c). The electrodes are powered by a capacitor bank with typical voltages of 3–10 kV and up to 50 kJ of stored energy. A double feedthrough is used to minimize the circuit inductance. Large DC coils outside the vacuum vessel provide

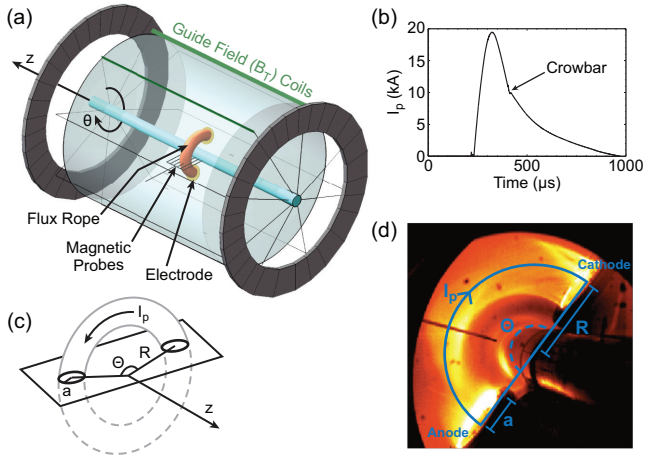

FIG. 1. (a) A schematic of the experimental setup. A plasma arc (orange) is maintained by two electrodes. Current through the center coil (center blue and return paths green) provides the toroidal guide magnetic field, B_T, along the plasma arc; one pair of external DC coils (big gray circles) provides the equilibrium field (B_E) along z direction. The current flowing in the plasma arc provides the poloidal field component that twists the field lines in the flux rope. Also shown is the 2D magnetic probe array. The plasma flux rope has a 20 cm major radius and is far away from the vacuum walls. (b) A typical plasma current waveform $I_p(t)$. (c) A schematic of the current loop with minor radius a and major radius R. (d) Visible image of plasma flux rope taken by a fast frame rate camera with 1 μs exposure.

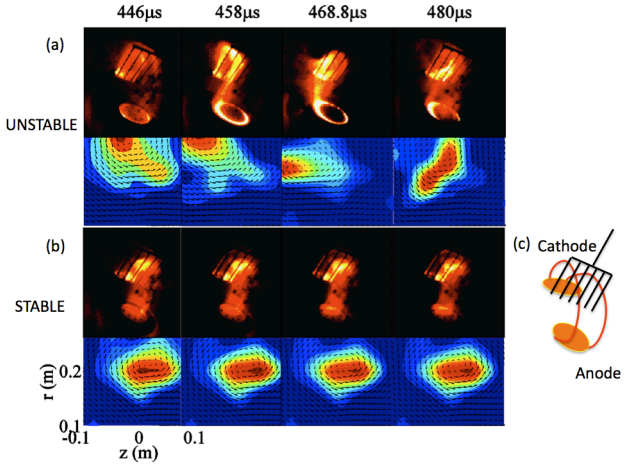

FIG. 2. Two hydrogen plasma shots with different toroidal guide field strengths. The images show visible light snapshots taken with a fast framing camera (color is added later). The vectors and contour plots show the poloidal magnetic field and the current density, respectively, as measured by the the 90-channel probe. (a) Unstable case. (b) Stable case. (c) Drawing of the plasma arc, electrodes, and 90-channel probe as seen in the fast camera images.

a z-directed strapping (equilibrium) field of up to 200 G that is largely uniform in space. A toroidal guide field B_T (along θ) of variable strength is applied using eight three-turn TF coils that are powered by a separate 0.5 F, 450 V capacitor bank. This system provides a toroidal field of 0–1500 G at the center of copper electrodes. The working gas is puffed in before the plasma is formed and fills the vacuum vessel to a uniform pressure. The gas can be injected through several PV-10 gas valves on the machine wall or through small holes in the electrodes. This configuration permits the use of a mixture of gases to achieve ionization at lower applied voltages. The discharges are monitored with a variety of magnetic probes, including a 2D (z-r) 90-channel probe array at one toroidal location and several additional 1D (radial) probes at various other toroidal locations. The magnetic signals are digitized at 2.5 MHz. Additionally, a fast CCD camera is used for monitoring the 3D evolution of the discharge in the visible spectrum. Frames can be captured every 4–12 μs with a 1 μs exposure time.

A typical discharge lasts about 700 μs (Fig. 1b). Figure 2 shows two discharges with different stability properties. The top panels are visible light snapshots taken at four different times by the fast framing camera (a false color map is added later). The bottom panels show the corresponding poloidal magnetic field measurements and the resulting current density obtained from the 90-channel probe. When the toroidal field strength is low, the flux rope kinks violently (Fig. 2a); however, with a stronger toroidal field the flux rope maintains a stable equilibrium and does not move around (Fig. 2b). Note that the visible light amplitude correlates well with the current density. Fast framing camera movies with the complete evolution of the flux rope show that a kink unstable flux rope makes rigid body rotations. The rotation frequency varies between 30–90 KHz depending mainly on the plasma current and the flux rope length. The rotation is most likely driven by plasma flows.

In order to examine the stability properties of these flux ropes more quantitatively, we can look at magnetic fluctuations that are measured by the 90-channel magnetic probe. In particular, we examine signals from individual magnetic pickup coils that are located near the edge of the 90-channel probe. These edge coils remain outside of the flux rope for the duration of the discharge and therefore measure only external magnetic fluctuations from the plasma. A sample fluctuating signal of poloidal magnetic field (δB_p) is plotted in black in each panel of Fig. 3. It is clear from these signals that the external magnetic fluctuations persist until a certain stabilization threshold is crossed where the plasma quickly ceases its kinking motion.

We next calculate the time evolution of the edge q value over the course of the discharge. This permits the identification of a threshold q value for each discharge (i.e., the q value at the time of stabilization). In order to calculate the edge q values for a given discharge, the various quan-

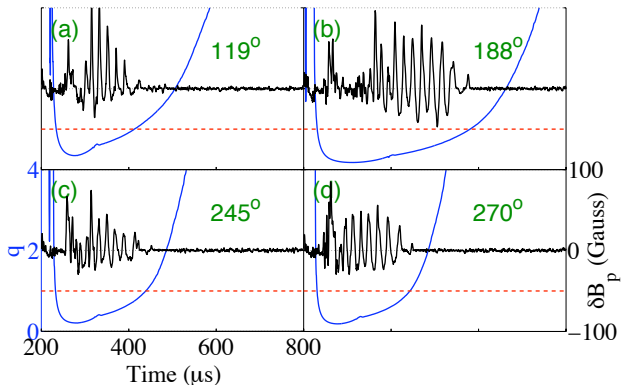

FIG. 3. Time evolution of the edge q value (blue, left axis) and magnetic fluctuation amplitude (black, right axis) for several flux ropes of varying arc length with $a = 7.3$ cm and $R \approx 19.5$ cm. The KS stability threshold ($q = 1$) is drawn in red. The fluctuation traces are taken from one of the pickup coils in the 2D 90-channel probe array that is near the edge of the plasma. The fluctuations that result from the external kinking and rotation of the plasma column stop when $q \simeq 1$.

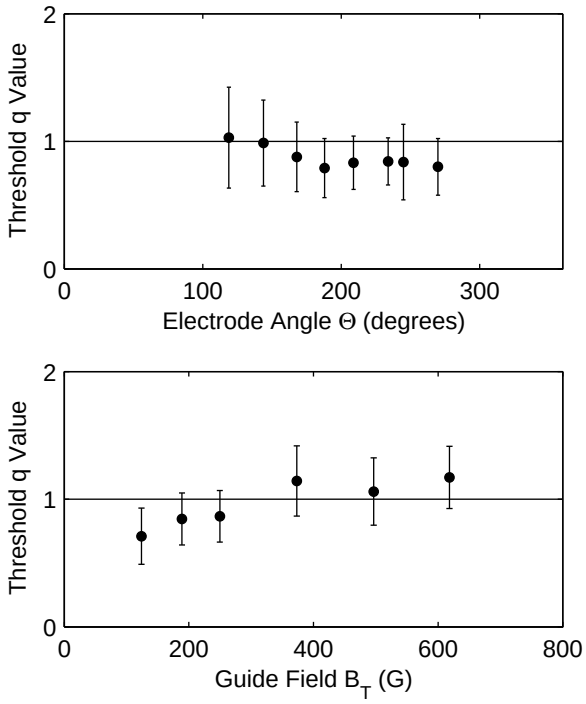

FIG. 4. (a) The measured threshold q value as a function of electrode separation angle Θ. Here $B_T = 120$ G and $a = 7.3$ cm. The black solid line marks the $q = 1$ Kruskal-Shafranov limit. (b) The measured threshold q value as a function of guide field strengh B_T. Here the electrode angle is $\Theta = 270°$ and again $a = 7.3$ cm. The error bars are calculated by combining the uncertainty in the individual threshold q measurements with the statistical variation over multiple shots.

tities in Eq. 1 must be collected. For this we assume that flux rope minor radius a is given by the electrode minor radius and that the toroidal field B_T is given by the guide field strength at the center of the electrodes. The plasma current waveform $I_p(t)$ is measured by a current transformer and the flux rope length waveform $L_p(t)$ is measured by various toroidally-distributed magnetic probes. For a detailed discussion of the length measurements, see the next section on equilibrium analysis. The resulting q evolution for each discharge is plotted in blue in Fig. 3. The four panels in Fig. 3 contain signals from discharges with different electrode angles (i.e., different flux rope lengths). Note that the rope stabilizes at a different time in each case, but that this time is always near $q \simeq 1$. In many cases, the stabilization time can also be verified by changes in the fast camera images.

We would now like to test the applicability of the Kruskal-Shafranov limit introduced earlier in this paper to the flux ropes produced in MRX. This is done by independently scanning the various quantities that modify the safety factor q. Since the plasma current I_p is scanned within each discharge by the rise and fall of the current waveform, we focus here on scans of the electrode separation angle Θ (which changes the flux rope length) and of the guide field B_T. The collection of threshold q values obtained from these parameter scans is shown in Fig. 4. It is clear that in both cases the stabilization threshold remains close to $q = 1$ throughout the scans. This serves to verify that the Kruskal-Shafranov theory captures the key physics of the stability of these flux ropes. It also supports the assertion that these flux ropes are line-tied to both of the electrodes. As mentioned, if the anode were instead free to move due to the presence of a resistive sheath, then the stabilization threshold would be $q = 2$. This is clearly not the case here. It is worth noting that if *both* ends of the flux rope are free to move, the stabilization threshold would again be $q = 1$. We are able to rule out this possibility, however, by examining the envelope of the measured kink oscillations. Thus we conclude that these flux ropes obey the $q > 1$ Kruskal-Shafranov limit for non-periodic line-tied flux ropes.

In addition to studying their stability properties, it is also interesting to study the MRX flux ropes' evolving radial equilibrium. We do this by installing 1D (radial) magnetic probes at up to 7 toroidal locations between the electrodes. Each of these probes measures B_z at several locations along its length, so the radial position of the flux rope can be determined by finding where the measured $B_z(r)$ profiles reverse sign. The radial position measurements are then used to reconstruct the evolving toroidal profile of the flux rope $R_p(\theta, t)$. The time evolution of R_p at a single toroidal location ($\theta = 337°$) is shown in Fig. 5a. This signal contains both a slowly-evolving equilibrium component and a faster fluctuating component that appears during the unstable phase of the discharge. The equilibrium expansion of the flux

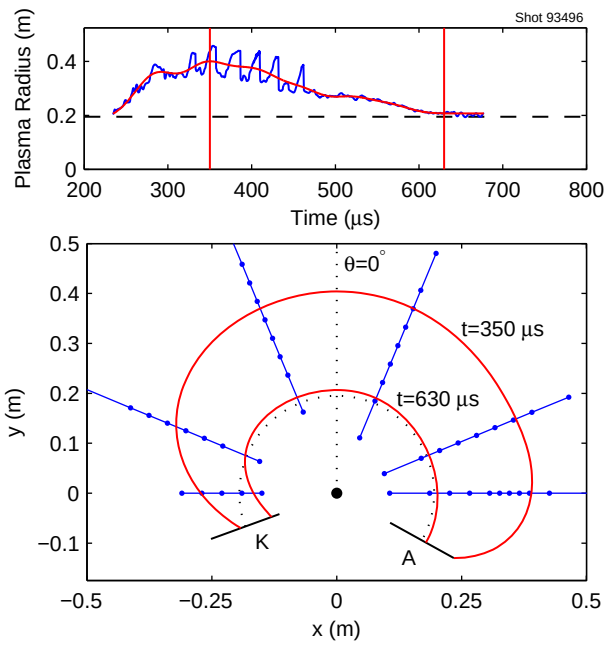

FIG. 5. (a) Time evolution of the plasma's major radius measured at one toroidal location (blue line) and the equilibrium radius around which the flux rope oscillates (red line). The horizontal dashed line marks the electrode major radius. (b) The toroidal profile of the flux rope at two times (which are marked by the vertical dashed lines in (a)). The larger-radius profile corresponds to the earlier (higher current) time. The blue lines/dots indicate the location of magnetic probes/coils and the black dotted line shows the electrode major radius.

rope can be examined by filtering out these faster fluctuations. The resulting spatial equilibrium profile $R_p(\theta)$ at two different times during the discharge is shown in Fig. 5b. Here, the radial position of the flux rope is extrapolated to the electrodes and then spline fitted to give a smooth rope profile. It is clear that the MRX flux ropes expand outwardly in analogy with line-tied coronal flux ropes. Additionally, by integrating along the toroidal profile, the rope length L_p can be determined for use in the q calculations described in the previous section.

The expansion and contraction of the flux rope equilibrium is a result of competing radial forces in the plasma. The primary forces at work are the current-driven hoop force, the strapping field force, and the force from tension in the toroidal magnetic field. While the latter two forces push inward, the hoop force pushes outward. One crucial observation with the MRX flux rope equilibria is that regardless of the strength of the strapping field, the current continues to flow in the plasma. In fact, no discharge was observed where the flux rope was entirely blown away. This is in stark contrast to tokamaks which rely on precise control of the vertical (strapping) field to maintain the discharge. The forces responsible for the maintenance of the flux rope discharge in the MRX experiments are thus an interesting subject for future study.

In summary, the stability and equilibrium characteristics of laboratory partial-toroidal flux ropes have been examined. The experimental results clearly show that the external kink stability threshold is governed by the Kruskal-Shafranov limit for a line-tied partial toroid ($q = 1$). The radial equilibrium properties of these flux ropes were also studied. It was found that, though the plasma expands radially and often kinks wildly, it is never blown away and always restabilizes at sufficiently low current. This suggests that non-linear saturation mechanisms for the external kink mode could be studied in the future using this experimental setup.

* eoz@princeton.edu; Present address: TeleSecurity Sciences, Inc., 7391 Prairie Falcon Road, Suite 150-B, Las Vegas, NV 89128, USA.
† myamada@pppl.gov
‡ Present address: CAS Key Laboratory of Plasma Physics, Department of Modern Physics, University of Science and Technology of China, Hefei 230026, China.

[1] M. Yamada, H. Ji, S. Hsu, T. Carter, R. Kulsrud, N. Bretz, F. Jobes, Y. Ono, and F. Perkins, Phys. Plasmas, **4**, 1936 (1997).
[2] N. Crooker, J. Joselyn, and J. Feynman, eds., *Coronal Mass Ejections* (American Geophysical Union Monograph 99, 1997).
[3] T. Forbes, J. Geophys. Res., **95**, 11919 (1990).
[4] B. Low, Solar Phys., **167**, 217 (1996).
[5] Z. Mikic and J. Linker, Astrophys. J., **430**, 898 (1994).
[6] S. Antiochos, C. DeVore, and J. Klimchuk, Ap. J., **510**, 485 (1999).
[7] P. A. Isenberg and T. G. Forbes, The Astrophysical Journal, **670**, 1453 (2007).
[8] M. Kruskal and J. L. Tuck, Royal Society of London Proceedings Series A, **245**, 222 (1958).
[9] V. Shafranov, At. Energy, **5**, 38 (1956).
[10] J. Wesson, *Tokamaks* (Clarendon Press, Oxford, 1987).
[11] I. Lanskii and A. Shchemikov, Sov. J. Plasma Phys., **16**, 322 (1990).
[12] C. Hegna, Phys. Plasmas, **11**, 4230 (2004).
[13] D. D. Ryutov, I. Furno, T. P. Intrator, S. Abbate, and T. Madziwa-Nussinov, Phys. Plasmas, **13**, 2105 (2006).
[14] S. C. Hsu and P. M. Bellan, Phys. Rev. Lett., **90**, 215002 (2003).
[15] W. F. Bergerson, D. A. Hannum, C. C. Hegna, R. D. Kendrick, J. S. Sarff, and C. B. Forest, Phys. Rev. Lett., **101**, 235005 (2008).
[16] I. Furno, T. P. Intrator, D. D. Ryutov, S. Abbate, T. Madziwa-Nussinov, A. Light, L. Dorf, and G. Lapenta, Physical Review Letters, **97**, 015002 (2006).
[17] X. Sun, T. P. Intrator, L. Dorf, I. Furno, and G. Lapenta, Physical Review Letters, **100**, 205004 (2008).
[18] J. Hansen and P. Bellan, Astrophys. J., **563**, L183 (2001).
[19] S. K. P. Tripathi and W. Gekelman, Phys. Rev. Lett., **105**, 075005 (2010).

The Princeton Plasma Physics Laboratory is operated
by Princeton University under contract
with the U.S. Department of Energy.

Information Services
Princeton Plasma Physics Laboratory
P.O. Box 451
Princeton, NJ 08543

Phone: 609-243-2245
Fax: 609-243-2751
e-mail: pppl_info@pppl.gov
Internet Address: http://www.pppl.gov